NJC

Accepted Manuscript

Volume 40 | Number 1 | January 2016 | Pages 1–846

NJC

New Journal of Chemistry
www.rsc.org/njc

A journal for new directions in chemistry

ISSN 1144-0546

ROYAL SOCIETY
OF CHEMISTRY

PAPER
Jason B. Benedict et al
The role of atropisomers on the photo-reactivity and fatigue of
diarylethene-based metal–organic frameworks

CΠГS

This is an Accepted Manuscript, which has been through the Royal Society of Chemistry peer review process and has been accepted for publication.

Accepted Manuscripts are published online shortly after acceptance, before technical editing, formatting and proof reading. Using this free service, authors can make their results available to the community, in citable form, before we publish the edited article. We will replace this Accepted Manuscript with the edited and formatted Advance Article as soon as it is available.

You can find more information about Accepted Manuscripts in the author guidelines.

ROYAL SOCIETY
OF CHEMISTRY

rsc.li/njc

Journal Name

ARTICLE

Pd nanoparticles immobilized on halloysite decorated with cyclodextrin modified melamine-based polymer: a promising heterogeneous catalyst for hydrogenation of nitroarenes

Samahe Sadjadi[*a], Maryam Akbari[b], Eric Monflier[c], Majid, M. Heravi[b], Bastien Leger[c]

For the first time, a hybrid system, composed of halloysite (Hal), cyclodextrin modified melamine-based polymer is developed and employed for immobilization of Pd(0) nanoparticles. The resulting catalytic hybrid system, Pd@HTMC, was then applied as a heterogeneous catalyst for hydrogenation of nitroarenes to the corresponding anilines. The results established that Pd@HTMC could promote hydrogenation under very mild reaction conditions and relatively short time. Moreover, investigation of sterically demanding substrate, nitro-naphthalene, as well as substrate with competing functional group, 4-nitroacetophenone, confirmed that the catalyst is capable of hydrogenation of sterically demanding substrate, while selectively hydrogenates nitro functional group over keto-functionality. The recyclability experiment proved that the catalyst was recyclable up to six reaction runs with slight loss of the catalytic activity and Pd leaching. Moreover, hot filtration test confirmed the heterogeneous nature of the catalyst. Finally, the contribution of cyclodextrin modified melamine-based polymer to the catalysis was confirmed by comparison of the catalytic activity of Pd@HTMC with control catalysts.

Introduction

Hal, is a natural dioctahedral 1:1 layered aluminosilicate $(Al_2Si_2O_5(OH)_4 \cdot nH_2O)$ with chemical and physical properties similar to kaolin. Hal possesses tubular morphology with Al-OH octahedral sheet groups on the inner and Si-O-Si groups on the outer surface [1-3]. The layers of Hal are separated with a monolayer of water molecules. The exterior surface of Hal is negatively charged, while the interior lumen is positively charged [4]. Besides the exceptional tubular morphology, Hal benefits from other advantages, including high thermal and mechanical resistance, availability, non-toxic nature, biocompatibility, high surface area and the capability of both inner and outer surface modification [5-7]. These features render Hal a promising candidate for versatile fields [8] such as packing, adsorbents, and polymer fillers, drug delivery [9], flame retardancy, energy storage and more importantly catalysis [10]. Recently, many attempts have been devoted to establish the catalytic application of pristine and functionalized Hal [10]. In this line, both experimental and theoretical studies confirmed that functionalities on the surface of Hal played an important role in the catalytic performance of the final catalyst [11-13].

Cyclodextrins, CDs, are cone-shape cyclic oligosaccharides with hydrophobic cavity and hydrophilic exterior [14]. α, β and γ-CDs possess 6, 7 and 8 glucopyranoside units respectively. Among various CDs, β-CD is of great interest due to its cavity size and relatively low cost [15, 16]. CDs are not only non-toxic and biocompatible, but also capable of formation of inclusion complex with various guest molecules with proper size and polarity. To date, CDs have been applied for diverse range of applications such as synthesis of nanomaterials, food industry, drug delivery and catalysis [17-23]. Among various applications, use of CDs in catalysis has been intensively focused [19, 22, 24]. Notably, CD can act as a molecular transfer shuttle and facilitate the conversion of the substrates at the aqueous/organic interface [25, 26].

Anilines are versatile fine chemicals, useful for the production of agrochemicals and antipyretic drugs, dyes, pigments, and pesticides [27, 28]. Conventionally, the amine derivatives are produced by the catalytic hydrogenation of nitro compounds, mostly in the presence of noble metal-based catalysts. Various homogeneous and heterogeneous catalysts have been reported for this process. However, due to the ever-increasing environmental standards and economic pressures, heterogeneous catalysts are mostly preferred for their easy separation, recovery and recyclability. In the case of heterogeneous catalysts, the consciously selection of support is an important issue, because the interaction between the

[a] Gas Conversion Department, Faculty of Petrochemicals, Iran Polymer and Petrochemicals Institute, PO Box 14975-112, Tehran, Iran. Tel.; +982148666; Fax; +982144787021-3; E-mail: samahesadjadi@yahoo.com and s.sadjadi@ippi.ac.ir
[b] Department of Chemistry, School of Science, Alzahra University, PO Box 1993891176, Vanak, Tehran, Iran. Tel.: +98 21 88044051; fax: +982188041344
[c] Univ. Artois, CNRS, Centrale Lille, ENSCL, Univ. Lille, UMR 8181, Unité de Catalyse et de Chimie du Solide (UCCS), F-62300 Lens, France.

support and the immobilized catalytically active metallic nanoparticles can affect distribution, size, activity and stability of the nanoparticles [29-31]. To date, immobilization of hydrogenation catalysts on the various supports such as activated carbon, silica, carbon nanotubes, clay and nanofibers have been disclosed [32-38]. Although the reported catalytic routes have provided significant achievements for the hydrogenation reaction, some of the methods are plagued by some limitations in terms of yields, low catalyst recovery, long reaction times, excess of organic solvent, high temperatures and harsh reaction conditions. Therefore, the design of new material is demanded to overcome these problems.

Following our research on development of heterogeneous catalysts [39, 40], recently, we focused on the functionalization of Hal and studied its utility as a heterogeneous support for immobilization of various catalytic active species ranging from heteropolyacids [41] to nanoparticles [42, 43]. Moreover, the results of studying the hybridization of CD and its polymers proved that introduction of CD and its derivatives can improve the catalytic performance of the hybrid systems due to the capability of formation of inclusion complex with substrate and exerting synergistic effect [42-44]. On the other hand, our recent studies revealed that incorporation of carbon-based materials such as graphitic carbon nitrides can effectively suppress leaching of the catalytic active species and enhance the catalytic activity and recyclability of the hybrid system [43].

Considering the possible synergism between Hal, CD and carbon porous materials, we designed and synthesized a triply hybrid system composed of Pd, Hal, and CD-modified melamine based polymer. It was assumed that due to the presence of CD in the structure of this heterogeneous catalyst, it could promote the reactions in aqueous media via formation of inclusion complex with substrates. Moreover, it was believed that melamine based polymer that is a porous polymer with multiple nitrogen atoms could increase Pd anchoring and decrease its leaching through electrostatic interactions. To verify these assumptions, the catalytic activity of Pd@HTMC for a model reaction, i.e. hydrogenation of nitrobenzenes to the corresponding anilines was targeted. Moreover, to elucidate the role of CD and melamine-based polymer, control catalysts (the catalysts without CD and melamine) were synthesized and their catalytic activities were compared with that of the catalysts. To investigate the generality of the reaction, the hydrogenation of sterically demanding substrate, nitronaphthalene, as well as substrate with competing functional group, 4-nitroacetophenone, was also investigated. Finally, the recyclability of the catalyst, Pd leaching as well as the heterogeneous nature of the catalysis was examined.

Eexperimental

Materials and instruments

All chemicals and reagents, including nitrobenzene, 1-nitronaphtalene, 4-nitroacetophenone, formic acid, sodium borohydride, halloysite clay (Hal), (3-chloropropyl) trimethoxysilane, thiosemicarbazide, melamine,

terephthaldehyde (TPA), potassium persulfate, β-cyclodextrin (β-CD), $Pd(OAc)_2$, toluene, dimethyl sulfoxide (DMSO) were analytical grade reagents, purchased from Sigma-Aldrich and were used without further purification. Catalyst characterization was carried out by applying various techniques, including TEM, XRD, BET, TGA, FTIR and ICP-AES. TEM was performed on a Tecnai microscope (200 kV). To perform the analysis, the samples were dispersed in water and the analysis was carried out after evaporation of the solvent. XRD patterns of the catalyst, pristine Hal and HTMC were obtained by using a Siemens, D5000. Cu Kα radiation from a sealed tube. The BET analyses of the pristine Hal and the final catalyst were performed using BELSORP Mini II instrument. Prior to analysis the samples were pre-heated at 200 °C for 3h. To perform thermogravimetric analysis (TGA) METTLER TOLEDO thermogravimetric analysis apparatus was employed. The applied heating rate was 10 °C min^{-1} and the analysis was carried out under N_2 atmosphere over the range of 50 to 800 °C. FTIR spectra were recorded by employing PERKIN-ELMER-Spectrum 65 instrument and ICP analyses were accomplished by using ICP analyzer (Varian, Vista-pro).

Synthesis of Hal-Cl

Hal-Cl was synthesized according to the previous report [11]. Typically, Hal (4 mmol, 1.2 g) was dispersed in 60 mL dry toluene via ultrasonic irradiation of power 100 W and subsequently (3-chloropropyl) trimethoxysilane (15 mmol) was added drop wise. The mixture was left under constant stirring for 24 h at 110 °C. Upon completion of the reaction, the precipitate was separated by simple filtering. The functionalized clay was obtained by repeated washing with dried toluene and drying at 100 °C overnight.

Synthesis of Hal-T

Typically, thiosemicarbazide (6.6 mmol) was added to a suspension of Hal-Cl (1 g) in toluene (50 mL) in the presence of catalytic amount of triethylamine (1 mL). The resulting mixture was then refluxed at 110° C for 24 h. Upon completion of the reaction, the precipitate was filtered off and washed several times with toluene and dried at 100 °C overnight.

Synthesis of melamine-based polymer on the surface of Hal-T: synthesis of (HTM)

The introduction of melamine-based polymer on Hal-T was achieved through the previous report [45]. Briefly, a mixture of Hal-T (3 g), melamine (4 mmol), terephthalaldehyde (9 mmol) in DMSO (50 ml) was prepared in a flask. The aforementioned mixture was then heated to 180 °C for 48 h under nitrogen atmosphere. After cooling to room temperature, the solid product was isolated by simple filtration, washed with acetone and water and dried at 60 °C.

Modification of HTM with CD: synthesis of HTMC

The modification of melamine-based polymer with β-CD was performed via the facial solvothermal method, reported previously [46]. Briefly, aqueous suspension of HTM (2 g in 12 mL of distilled water) was mixed with a solution of β-

cyclodextrin (0.7 mmol CD in 8 mL of distilled water) at room temperature. In the following, 0.2 ml of NaOH solution (1 M) and 0.037 mmol potassium persulfate ($K_2S_2O_8$) as an initiator were added. The mixture was then stirred until the suspension became clear. Subsequently, it was transferred into an autoclave, sealed and heated to 180 °C and maintained for 12 h at this temperature. Upon completion of the reaction, the resulting participate was washed with distilled water and ethanol several times, and dried in vacuum at 60 °C.

Synthesis of Pd@ HTMC

The catalyst, Pd@HTMC, was prepared by incorporation of Pd nanoparticles via wet impregnation method. Briefly, HTMC (1.2 g) was dispersed into 30 mL of dry toluene containing 0.09 mmol Pd(OAc)$_2$ in 12 mL toluene. The mixture was stirred at room temperature for 8 h. Subsequently a solution of NaBH$_4$ in MeOH (10 mL, 0.2 N) was added into the suspension dropwise and the resulting mixture was stirred for 2 h. Finally, the solid material was filtered off, washed with MeOH and dried in oven at 60 °C for 12 h. The schematic procedure of the synthesis of the catalyst is illustrated in Figure 1.

Pd loading of Pd@HTMC was measured via ICP-AES analysis. First, a mixture (1:5) of concentrated nitric and hydrochloric acid (6 M) was prepared and a known amount of Pd@HTMC (0.002 g) was digested in the aforementioned acidic solution through constant stirring for 8 h. Subsequently, the resulting extract was analyzed by ICP-AES. The Pd content of the catalyst was measured to be about 0.45 wt%.

General procedure for the hydrogenation of nitro compounds

In a typical reaction, the mixture of nitroarene compounds (1 mmol) and the Pd@HTMC catalyst (1 wt %) in deionized water (2 mL) were placed into a reactor and heated up to 50 °C. Then, hydrogen (1 bar) was purged into the flask continuously and the mixture was stirred vigorously (800 rpm). Upon completion of the reaction (monitored by TLC), the resultant mixture was filtered to separate the catalyst and the product was isolated by evaporation of solvent and identified by comparing its boiling/melting point and FTIR spectrum with that of the authentic sample. To recycle the catalyst, the recovered Pd@HTMC was washed with water and dried at 100 °C overnight.

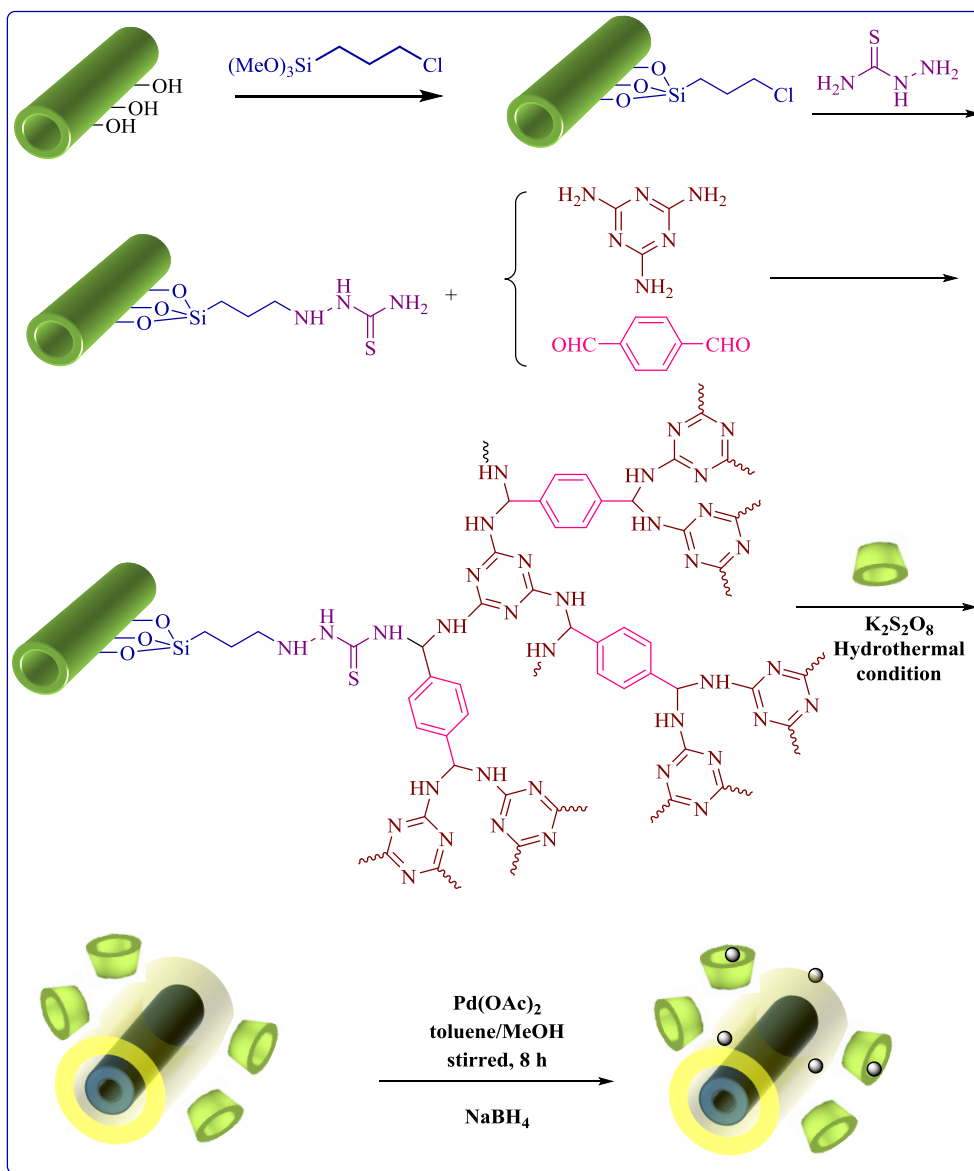# Journal Name

ARTICLE

Figure 1. The schematic procedure of the synthesis of the catalyst.

Result and discussion

Catalyst Characterization

As described in the Experimental section, the catalyst, Pd@HTMC, was prepared through functionalization of Hal with

thiosemicarbazide and formation of melamine-based polymer and its modification of CD, followed by immobilization of Pd(0) nanoparticle. The TEM images of Pd@HTMC is depicted in Figure 2. As shown, the tubular morphology of Hal can be detected in these images, indicating that the morphology of Hal did not collapse by incorporation of CD-modified

melamine-based polymer. However, the comparison of the morphology of pristine Hal with that of the catalyst (Figure S1), imply that the diameters of the pristine Hal tubes is lower than that of Pd@HTMC. This observation can be attributed to the coverage of Hal surface with CD-modified melamine-based polymer. In the TEM images of the catalyst the fine sheets of CD-modified melamine-based polymer can be observed. Moreover, Pd nanoparticles are depicted as dark spots. As shown in Figure 2, in some part, Pd nanoparticles are aggregated. Using TEM images the average size of Pd nanoparticles was estimated to be 7±0.1 nm.

The structural feature of Pd@HTMC was studied by recording FTIR spectrum of the catalyst and comparing it with that of Hal, Hal-Cl, Hal-T, HTM and HTMC (Figure 3). The characteristic bands of Hal include the bands at 3695 cm^{-1} and 3627 cm^{-1} (representing the internal hydroxyl group of Hal), the bands at 534 (indicative of Al-O-Si vibration) and 1033 cm^{-1} (Si–O stretching) [47]. The FTIR spectrum of Hal-Cl is very similar to that of pristine Hal and exhibit all the characteristic bands of Hal, indicating that the structure of Hal is not destructed after functionalization with organosilane. The spectrum of Hal-T also contained the representative bands of Hal. Furthermore, the FTIR spectrum of Hal-T showed some additional bands, i.e., a band at 1302 cm^{-1} that can be attributed to C=S group in thiosemicarbazide and the bands at 3260 and 3384 cm^{-1}, which are the representative of stretching and bending vibration of N-H and NH$_2$. In the FTIR spectrum of HTM, the amine bands of thiosemicarbazide functionality are disappeared, implying that this functionality participated in the polymerization reaction. Noteworthy, the characteristic band of C=N (1650 cm^{-1}) that are representative of melamine-based polymer overlapped with those of Hal. As depicted, modification of HTM with CD did not alter the FTIR spectrum dramatically. This observation is not beyond the expectation, as the characteristic bands of CD mostly overlapped with that of HTM. The FTIR spectrum of the catalyst, Pd@HTMC, is also similar to that of HTMC.

To investigate the structural features of the catalyst, the XRD pattern of Pd@HTMC was recorded (Figure 4). Additionally, to elucidate how hybridization of Hal with CD-modified melamine-based polymers as well as Pd immobilization can affect the structure of the Hal, the XRD patterns of the pristine Hal and HTMC were achieved and compared with that of the catalyst (Figure 4). The XRD pattern of pristine Hal is in good agreement with literature and exhibited the characteristic bands at 2θ = 11.8°, 19.9°, 24.8°, 26.5°, 36°, 38.5°, 55.3° and 62.5° (JCPDS No. 29-1487) [48, 49]. The XRD pattern of HTMC possessed the bands of Hal, indicating that incorporation of CD-modified melamine-based polymer did not result in collapse of Hal structure. However, the intensity of the bands reduced. Comparing the XRD pattern of pristine Hal with those of HTMC and Pd@HTMC, it can be concluded that no significant shift happened and the interlayer distance remained intact, implying that the functionalities as well as Pd nanoparticles are located on the surface, but not within the lumen of Hal. This issue was also verified in TEM images (Figure 2).

As depicted in the XRD pattern of Pd@HTMC, no additional bands were detected for Pd species. According to the literature, this observation can be attributed to the low loading of Pd, as also confirmed by ICP, and its high dispersion [50]. Pd@HTMC was also characterized by using BET. Considering the standard nitrogen adsorption–desorption types of isotherms, the isotherm of Pd@HTMC (Figure S2) can be assigned to type II isotherms with H3 hysteresis loops [49]. Moreover, the comparison of the isotherm of the catalyst with that of pristine Hal (Figure S3), established the similarity of two isotherms.
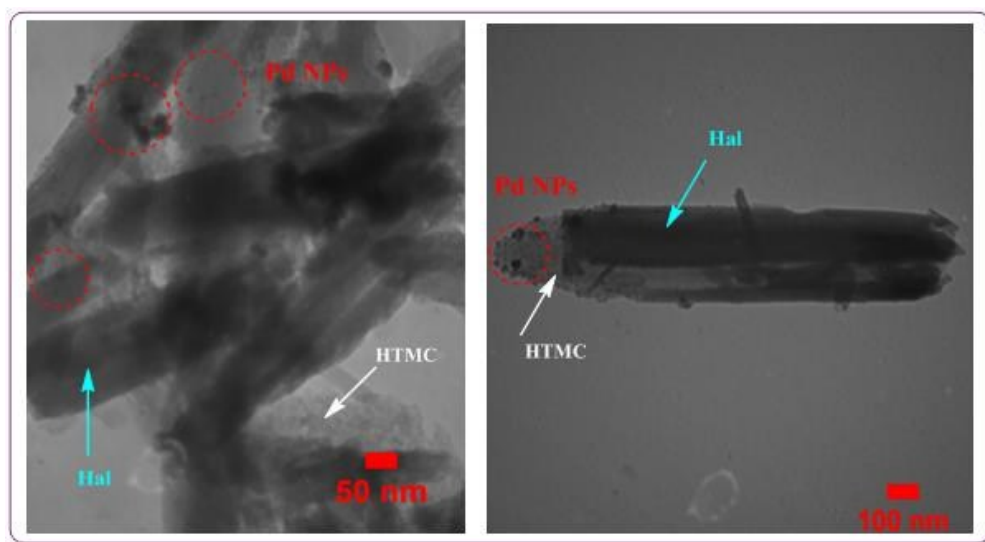

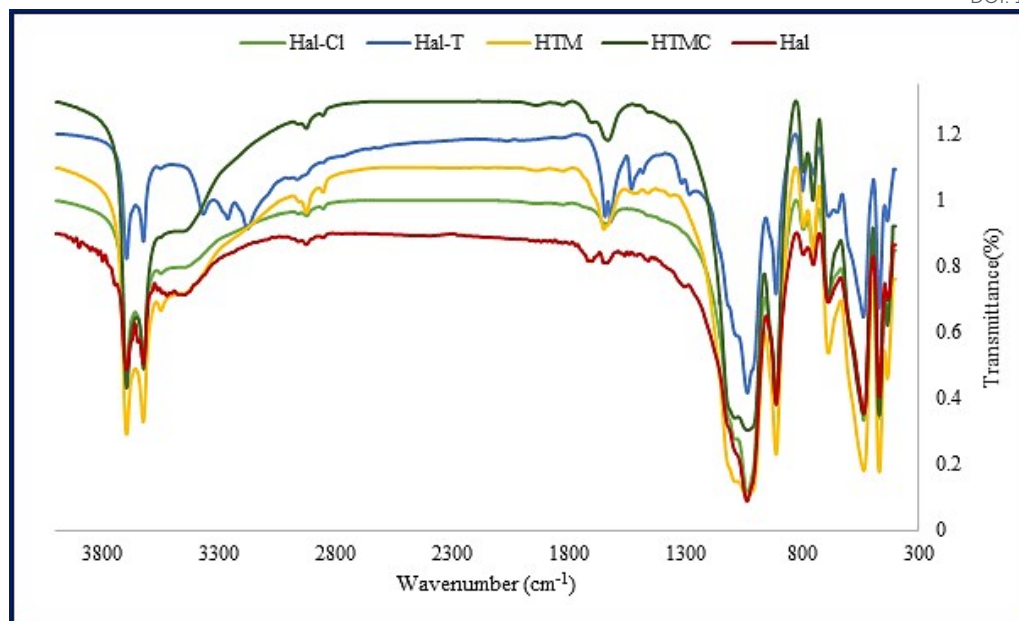
Figure 2. TEM images of Pd@HTMC.

ARTICLE

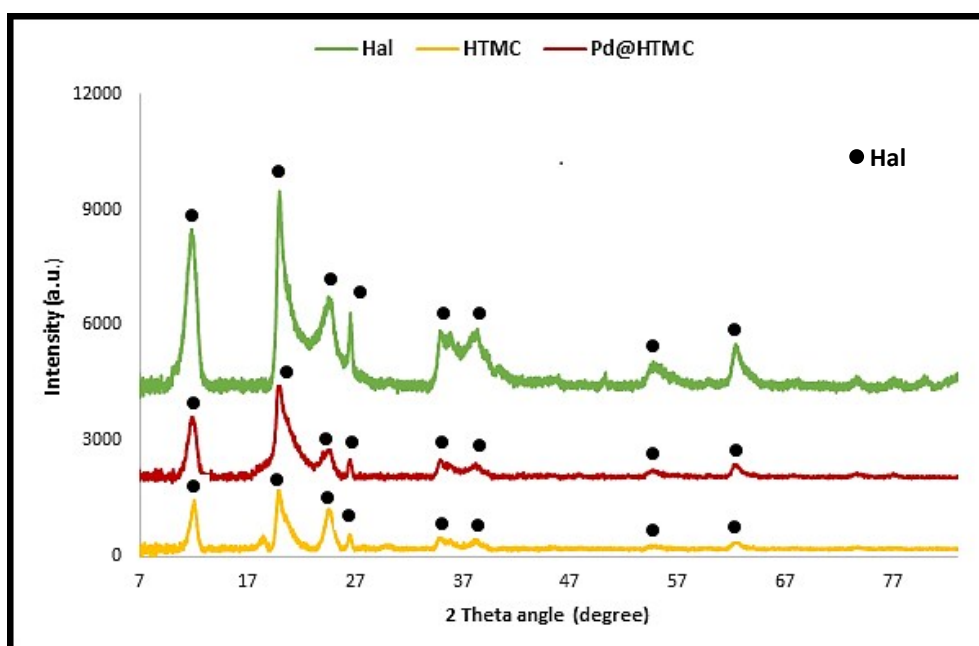**Figure 3.** FTIR spectra of pristine Hal, Hal-Cl, Hal-T, HTM, HTMC and Pd@HTMC.

Figure 4. XRD patterns of pristine Hal, HTMC and Pd@HTMC.

The specific surface area of Pd@HTMC was also calculated and compared with that of HTM, HTMC and Hal (Table 1). As tabulated, the specific area of Hal is 51 $m^2.g^{-1}$. Upon functionalization of Hal with melamine-based polymer the specific surface area of Hal decreased to 21.48 $m^2.g^{-1}$. This observation can confirm that melamine-based polymer was located on the surface of Hal. Moreover, the decrease in the surface area can be attributed to the large pores of melamine-based polymer [45]. As can be seen, upon modification of melamine-based polymer with CD, the specific surface area increased to 58.57 $m^2.g^{-1}$. The reason of this observation is that CDs could locate within the large cavities of melamine-based polymer. In the case of Pd@HTMC, the specific surface

area slightly decreased (52.63 m^2.g^{-1}). This can be attributed to embedment of Pd nanoparticles on the surface of HTMC.

Comparing total pore volumes of Hal, HTM, HTMC and Pd@HTMC, it was revealed that upon incorporation of melamine-based polymer, this value slightly increased (from 0.2 to 0.28 m^{3}g^{-1}). This observation can be attributed to the cavities

in the structure of melamine-based polymer [45]. Upon modification of melamine-based polymer with CD, this value increased to 0.38 m^{3}g^{-1}. This issue can be attributed to the presence of the cavities of CD. As expected, immobilization of Pd nanoparticles led to the decrease of the total pore volume. The pore diameters of Hal, HTM, HTMC and Pd@HTMC have also been compared. The results showed that upon incorporation of melamine based polymer this value increased from 5.42 nm (pristine Hal) to 28.65. As mentioned before, this observation can be attributed to the presence of large pores in melamine-based polymer [45]. Notably, modification of melamine-based polymer with CD resulted in decrease of this value to 5.42 nm. As indicated, this observation can be justified by considering the fact that CDs could place within the large pores of melamine-based polymer. As expected, incorporation of Pd resulted in decrease of this value, implying the embedment of Pd nanoparticles within the pores of the catalyst structure.

To further characterize the catalyst, the thermogram of Pd@HTMC was recorded (Figure 5). Additionally, to estimate the content of thiosemicarbazide, CD-modified melamine-based polymer, the thermograms of Hal, Hal-T and Hal-Cl were

Table 1.
Textural properties of Hal, HTM, HTMC and Pd@HTMC.

Sample	S_{BET} (m^2/g)[a]	V_t (m^3/g)[b]	$d_{BJH-KJS\ ads/des}$ (nm)[c]
Hal	51	0.2	5.42
HTM	21.48	0.28	28.64
HTMC	58.57	0.38	42
Pd@HTMC	52.63	0.26	3.28

[a] S_{BET} (BET surface areas), [b] V_t (total pore volume was estimated at a relative pressure of P/P_0=0.990, [c] $d_{BJH-KJS\ ads/des}$ (pore diameters derived from the adsorption/desorption branch by the BJH–KJS method).

also obtained (Figure 5). As illustrated in Figure 5, the thermogram of Hal exhibits two weight losses, at about 150 °C and 550 °C, that are due to the loss of water and

dehydroxylation of the Hal matrix respectively [51, 52]. Comparing the two thermograms of Hal-Cl and Hal, the amount of (3-chloropropyl) trimethoxysilane can be estimated to be ~3.3 wt%. To measure the content of thiosemicarbazide, thermogram of Hal-T was compared with that of Hal-Cl. The result showed that the content of T was about 4 wt%. Considering the thermogram of Pd@HTMC, the amount of CD-modified melamine-based polymer was estimated to be about 5.7 wt%.

Catalytic Activity of the Catalyst

In the next section, the catalytic activity of Pd@HTMC was assessed for the hydrogenation of nitro compounds. In an initial endeavour, synthesis of aniline from hydrogenation of nitrobenzene in the presence of hydrogen (1 bar) at 35 °C was examined. As employing green solvents for promoting organic reactions can modernize the classical procedures to make them more clean, safe and easy to perform, water was selected as a solvent. Gratifyingly, the reaction proceeded successfully to furnish aniline in high yield (Table 2). Encouraged by this result, finding the optimum reaction condition was targeted. In this line, the effects of several reaction variables such as the catalyst loading, temperature and hydrogen source on the yield of the model product were examined (Table 2). It is worth mentioning that use of lower hydrogen flow was not successful. On the other hand, increase of temperature from 35 to 50 °C could improve the yield of the reaction. Noteworthy, further increase of the temperature had a converse effect on the reaction yield, as at higher temperature the solubility of hydrogen would decrease in the solvent. Studying the effect of catalyst loading (0.5-10 wt%), it was found that 1 wt% was the optimum catalyst amount.

Next, the effect of hydrogen source was investigated by applying H$_2$ gas, formic acid and sodium borohydride as hydrogen source (Table 2, entries 9-10). Comparing the yields of the model product under the optimized reaction conditions, it was established that hydrogen gas was the best hydrogen source and led to the highest yield under mild reaction conditions. Thus, using 1 wt% Pd@HTMC catalyst and hydrogen gas as a hydrogen source at 50 °C in water was selected as the optimum reaction conditions for further investigations.

In the next step, the contribution of each component of the catalyst to the catalysis was studied. In this line, several control samples, including Hal-T, Pd@Hal-T, HTM, Pd@HTM, HTMC and Pd@HTM+CD were synthesized and their catalytic activity for hydrogenation of nitrobenzene to aniline under optimized reaction condition was studied and compared with that of Pd@HTMC, Table 3.
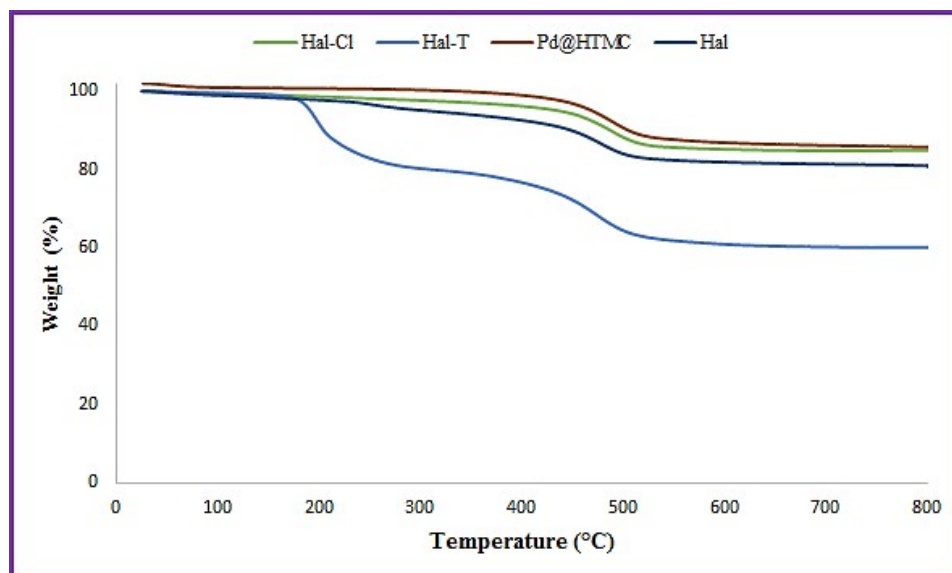
Journal Name

ARTICLE

Figure 5. The TGA analyses of pristine Hal, Hal-Cl, Hal-T and Pd@HTMC.

Table 2.
Effects of H_2 source, temperature, loading of catalyst on the yield of nitrobenzene hydrogenation reaction [a]

Entry	H_2 Source	Temp. (°C)	Catalyst [b](w/w%)	Yield (%)[c]
1	H_2 gas	35	10	50
2	H_2 gas	50	10	100
3	H_2 gas	50	7	100
4	H_2 gas	50	5	100
5	H_2 gas	50	3	100
6	H_2 gas	50	1	100
7	H_2 gas	50	0.5	60
8	HCOOH[d]	50	1	-
9	NaBH$_4$[e]	50	1	50

[a] Reaction condition: Nitrobenzene (1 mmol), H_2O (2 mL), hydrogen flow of 50 mL/min, agitation (800 rpm) in 1 h. [b] Pd loading of the catalyst is 0.45 wt%. [c] Isolated yields. [d] HCOOH (5 mmol, 0.2 ml). [e]NaBH$_4$ (5 mmol, 0.185 g).

Table 3.

Comparison of catalyst systems in hydrogenation of nitrobenzene [a]

Entry	Catalyst	Reaction time (h)	Yield (%)[b]
1	Hal-T	1	-
2	Pd@Hal-T	1	5
3	HTM	1	-
4	Pd@HTM	1	25
5	HTMC	1	-
6	Pd@HTMC	1	100
7	Pd@HTM+CD	1	50

[a] Reaction condition: Substrate (1 mmol), catalyst (1 wt%), H_2O (2 mL), hydrogen flow of 50 mL/min, agitation (800 rpm) at 50 °C in 1 h. [b] Isolated yields.

As expected, the Pd-free catalysts did not exhibit the catalytic activity and the reaction did not proceed in the presence of these catalysts. As tabulated, the catalytic activity of Pd@Hal-T after 1h was insignificant and only a trace amount of the desired product was obtained. In the case of Pd@HTM, the observed catalytic activity within 1h (yield = 25%) was higher than that of Pd@Hal-T, indicating the role of melamine-based polymer in the catalysis. It was assumed that the observed difference in the catalytic activity could stem from different Pd loading and Pd particle size of two control catalysts. To verify this assumption, the Pd particle sizes and loadings of Pd@Hal-T and Pd@HTM were measured by recording TEM images of two catalysts (Figure S4) and performing ICP analysis respectively. The results of ICP analysis showed that the Pd loading of the latter was almost two times higher than that of the former, indicating the role of HTM in anchoring Pd nanoparticles [53-56]. Moreover, the comparison of two TEM images confirmed that Pd@Hal-T showed more aggregated morphology (Figure 3S), in which Pd nanoparticles were mostly aggregated (average particle size of 18 nm). The Pd nanoparticles in Pd@HTM, however, were more dispersed and their average particle size was 10 nm. Hence, the higher catalytic activity of Pd@HTM compared to Pd@Hal-T can be attributed to higher dispersion and smaller size of Pd nanoparticles in Pd@HTM and its higher Pd content. According to the previous literature [43], higher Pd content in Pd@HTM can be justified on the base of the electrostatic interactions of nitrogen atoms on the polymeric sheet and Pd species.

Comparison of the catalytic activity of Pd@HTM and Pd@HTMC demonstrated that the catalytic activity of the latter was significantly superior to that of Pd@HTM, implying the contribution of CD to the catalysis. Considering the previous reports [57, 58], the contribution of CD can be discussed from two points of view. First, the capability of CD to form inclusion complex with hydrophobic substrate and transferring it to the aqueous reaction media. To further confirm this issue, the hydrogenation reaction of more hydrophobic substrate, 1-nitronaphthalene, was performed in the presence of CD-free catalyst, Pd@HTM. As expected, the reaction of 1-nitronaphthalene that is insignificantly soluble in aqueous media did not proceed even after 3 h. Secondly, CD can serve as a capping agent and stabilize Pd nanoparticles. This issue is very well established in the literature [22, 59-61]. More precisely, in

the course of reduction of Pd(II) to Pd(0), the CDs present on the structure of the catalyst could act as stabilizing agent and prevented Pd(0) nanoparticles from aggregation and consequently led to the formation of Pd(0) particles with smaller sizes. To confirm this issue the average Pd particle sizes of Pd@HTM and Pd@HTMC were compared. The results showed that the average particle size of Pd@HTMC (7 nm) was smaller than that of Pd@HTM (10 nm).

Finally, to elucidate whether modification of melamine-based polymer with CD in a hybrid system can lead to superior catalytic activity than use of CD and Pd@HTM as individual components, both Pd@HTM and CD were applied as catalysts for promoting the model reaction (Table 3 entry 7). Interestingly, use of Pd@HTM and CD led to lower yield of the desired product compared to the hybrid Pd@HTMC. This observation confirmed that hybridization of the two components resulted in a catalytic system with superior efficiency than that of separated components.

To explore the scope and limitations of this catalytic system, some other substrates with different steric and electronic properties were subjected to the hydrogenation reaction under the optimized reaction condition (Table 4). Surprisingly, use of sterically demanding 1-nitronaphtalene as substrate resulted in hydrogenated product, conversion 100%, in 2 h. Although the reaction time was relatively low, it was higher than nitobenzene. The observed longer reaction time can be attributed to the larger molecular size of 1-nitronaphtalene compared to nitrobenzene [62] that can retard formation of inclusion complex with CD. This observation can confirm the fact that the catalyst shows size selectivity to some extent and the substrate that can be encapsulated within the cavity of CD more easily tolerates the hydrogenation reaction faster.

Studying hydrogenation of 4-nitroacetophenone, a more challenging substrate containing two active functional groups, i.e. $-NO_2$ and $-C=O$, it was found that the catalyst could selectively hydrogenate nitro functional group, while remained the ketone functionality intact.

Catalyst recyclability

ARTICLE

Journal Name

In the next section, the recyclability of the catalyst was studied in hydrogenation of nitrobenzene under the optimized reaction condition. To this purpose, the efficiency of the fresh Pd@HTMC was compared with the recycled ones. To recycle the catalyst, Pd@HTMC was separated via simple filtration and after washing with water and drying in oven at 100 °C overnight, it was subjected to the next run of the reaction under the same reaction condition. The results of recycling of Pd@HTMC up to seven reaction runs are illustrated in Figure 6. As depicted, the catalyst exhibited high recyclability up to six consecutive reaction runs. More precisely, no loss of the catalytic activity was observed upon second use, while slight loss of the catalytic activity was detected upon further recycling. Notably, the efficiency of Pd@HTMC upon recycling for the 7th reaction runs dramatically decreased (only 45% yield of the desired product was achieved). To investigate the origin of this decrease in the yield of the product, the recycled catalyst was characterized via ICP analysis and FTIR spectroscopy. As shown in Figure 7, the FTIR spectrum of the recycled Pd@HTMC after 7th reaction run is very similar to that of the fresh Pd@HTMC, indicating that recycling of the catalyst did not result in the collapse of the structural feature of Pd@HTMC. The investigation of Pd leaching via ICP analysis however, showed that the Pd leaching can be affected by recycling. More precisely, no leaching was observed for the catalyst recycled for the second reaction run while insignificant Pd leaching was observed for the catalysts recycled for the third and fourth reaction runs. Leaching of Pd nanoparticles constantly increased upon further recycling and reached to the maximum amount at seventh recycling (2.3 wt% Pd content of the catalyst). Notably, to rule out the possibility of deposition of Pd nanoparticles on the hydrogenation product, aniline, the ICP analysis was also performed for the product. The result showed that no Pd was deposited on the product. Considering these results, the loss of the catalytic activity upon recycling can be attributed to the Pd leaching.

Finally, to investigate the nature of the catalysis, the hot-filtration test was performed via standard method [63]. Briefly, the catalyst was filtrated from the reaction mixture and the progress of the reaction mixture in the absence of the catalyst was monitored. The result demonstrated that the reaction did not proceed, ruling out the possibility of the leaching of Pd nanoparticles from the support and re-deposition on it in the course of the reaction.

Table 4.

Hydrogenation of nitro compound by Pd@HTMC [a]

Entry	Substrate	Time (h)	Conversion (%)	Yield (%)[b]
1	Nitrobenzene	1	100	100
2	1-Nitronaphthalene	2	100	100
3	4-Nitroacetophenone	1.5	100	100

[a] Reaction condition: Substrate (1 mmol), catalyst (1 wt%), H_2O (2 mL), hydrogen flow of 50 mL/min, agitation (800 rpm) at 50 °C. [b] Isolated yields.
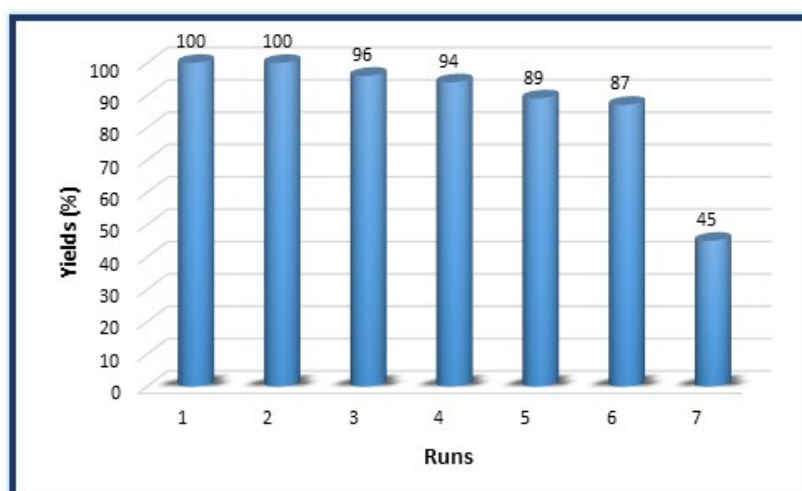

Figure 6. Recyclability of Pd@HTMC in the hydrogenation of nitrobenzene. Reaction condition: nitrobenzene (1 mmol), catalyst (1 wt%), H_2O (2 mL), hydrogen flow of (50 mL/min) at 50 °C.
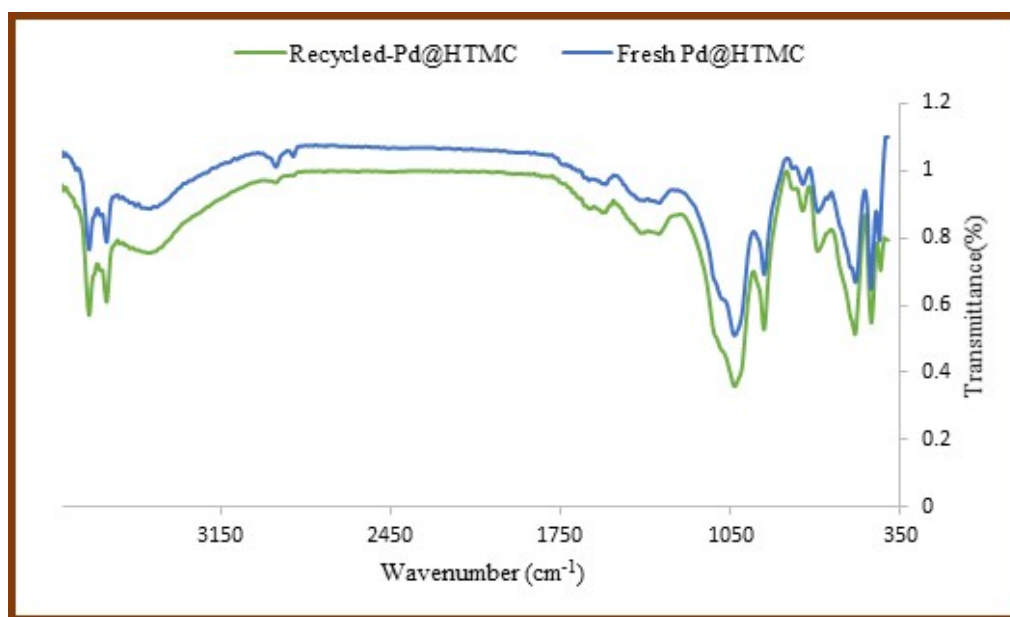
Figure 7. The FTIR spectra of fresh and recycled Pd@HTMC in the hydrogenation of nitrobenzene. Reaction condition: nitrobenzene (1 mmol), catalyst (1 wt%), H_2O (2 mL), hydrogen flow of (50 mL/min) at 50 °C.

Conclusion

A novel catalyst, Pd@HTMC, is prepared through growth of melamine-based polymer on the functionalized Hal followed by its modification with CD and Pd(0) nanoparticle immobilization. Pd@HTMC could successfully hydrogenate nitrobenzene and sterically demanding nitro-naphthalene in aqueous media. In the case of 4-nitroacetophenone that contained both nitro and ketone functionality, the catalyst selectively hydrogenated the nitro group. The comparison of the catalytic activity of the catalyst with that of, Pd@Hal-T and Pd@HTM confirmed the contribution of CD-modified melamine-based polymer to the catalysis. The results established that incorporation of melamine-based polymer could improve anchoring of Pd species through electrostatic interactions, while suppress the Pd leaching. The presence of CD on the structure of the catalyst, on the other hand, could promote formation of inclusion complex with hydrophobic substrate and transferring them into the aqueous media. Moreover, CD could act as a capping agent and stabilize Pd nanoparticles. The recyclability tests revealed high recyclability of the catalyst, up to six reaction runs, with slight loss of the catalytic activity and leaching of Pd. Moreover, hot filtration test confirmed the heterogeneous nature of the catalysis.

Acknowledgement

Notes and references

1.   P. Pasbakhsh and G. J. Churchman, *Taylor & Francis Group*, 2015.
2.   K. C. Christoforidis, M. Melchionna, T. Montini, D. Papoulis, E. Stathatos, S. Zafeiratos, E. Kordoulie and P. Fornasiero, *RSC Adv.*, 2016, **6**, 86617-86626.
3.   P. Liu and M. Zhao, *Appl. Surf. Sci.*, 2009, **255**, 3989–3993.
4.   W. Ma, H. Wu, Y. Higaki and A. Takahara, *Chem. Rec.*, 2018, **18**, 1-15.
5.   M. Massaro, S. Riela, P. Lo Meo, R. Noto, G. Cavallaro, S. Milioto and G. Lazzara, *J. Mater. Chem. B* 2014, **2**, 7732-7738.
6.   M. Massaro, V. Schembri, V. Campisciano, G. Cavallaro, G. Lazzara, S. Milioto, R. Noto, F. Parisi and S. Riela, *RSC Adv.*, 2016, **6**, 55312-55318.
7.   M. M. Massaro, S. Riela, G. Cavallaro, C. G. Colletti, S. Milioto, R. Noto, F. Parisi and G. Lazzara, *J. Mol. Catal. A.*, 2015, **408**, 12-19.
8.   G. Cavallaro, G. Lazzara, S. Milioto and F. Parisi, *Chem. Rec.* , 2018, **18**, 1-11.
9.   M. Massaro, S. Piana, C. G. Colletti, R. Noto, S. Riela, C. Baiamonte, C. Giordano, G. Pizzolanti, G. Cavallaro, S. Milioto and G. Lazzara, *J. Mater. Chem. B*, 2015, **3**, 4074-4081.
10.   M. Massaro, C. G. Colletti, G. Lazzara, S. Milioto, R. Noto and S. Riela, *J. Mater. Chem. A*, 2017, **5**, 13276–13293.
11.   S. Sadjadi, T. Hosseinnejad, M. Malmir and M. M. Heravi, *New J. Chem.*, 2017, **41**, 13935-13951.

ARTICLE   **Journal Name**

12. S. Sadjadi and N. Bahri-Laleh, *J. Porous Mater.*, 2017, In press.
13. N. Bahri-Laleh, S. Sadjadi, M. M. Heravi and M. Malmir, *Appl. Organomet. Chem.* .
14. S. Manivannan and R. Ramaraj, *Chem. Eng. J.*, 2012, **210**, 195-202.
15. L. Strimbu, J. Liu and A. E. Kaifer, *Langmuir* 2003, **19**, 483-485.
16. M. Jahjah, B. Caron, S. Menuel, E. Monflier, L. Djakovitch and C. Pinel, *ARKIVOC*, 2011, DOI: http://dx.doi.org/10.3998/ark.5550190.0012.733, 406-415.
17. S. Noël, B. Léger, A. Ponchel, K. Philippot, A. Denicourt-Nowicki, A. Roucouxd and E. Monflier, *Catal. Today*, 2014, **235**, 20-32.
18. S. Noël, B. Légera, A. Ponchel, F. Hapiot and E. Monflier, *Chem. Eng. Trans.*, 2014, **37**, 337-342.
19. L. Bai, F. Wyrwalski, J. F. Lamonier, A. Y. Khodakov, E. Monflier and A. Ponchel, *Appl. Catal., B.*, 2013, **138-139**, 381– 390.
20. A. Gogoi and K. C. Sarma, *Mater. Chem. Phys.*, 2017, **194**, 327-336.
21. S. Menuel, B. Léger, A. Addad, E. Monflier and F. Hapiot, *Green Chem.*, 2016, **18**, 5500-5509.
22. N. T. Thanh Chau, S. Handjani, J. P. Guegan, M. Guerrero, E. Monflier, K. Philippot, A. Denicourt-Nowicki and A. Roucoux, *Chem. Cat. Chem.*, 2013, **5**, 1497-1503.
23. B. Kaboudin, H. Salemi, R. Mostafalu, F. Kazemi and T. Yokomatsu, *J. Organomet. Chem.*, 2016, **818**, 195–199.
24. Q. Yi, L. Sun, X. Liu and H. Nie, *Fuel*, 2013, **111**, 88-95.
25. F. Hapiot, H. Bricout, S. Menuel, S. Tilloy and E. Monflier, *Catal. Sci. Technol.*, 2014, **4**, 1899-1908.
26. F. Hapiot and E. Monflier, *Catalyst*, 2017, **7**, 173.
27. T. Sugimura, K. Wakabayashi, H. Nakagama and M. Nagao, *Cancer Sci.*, 2004, **95**, 290-299.
28. H. U. Blaser, C. Malan, B. Pugin, F. Spindler, H. Steiner and M. Studer, *Adv. Synth. Catal.*, 2003, **345**, 103-151.
29. M. Cargnello, V. V. T. Doan-Nguyen, T. R. Gordon, R. E. Diaz, E. A. Stach, R. J. Gorte, P. Fornasiero and C. B. Murray, *Science*, 2013, **341**, 771-773.
30. G. Sevjidsuren, S. Zils, S. Kaserer, A. Wolz, F. Ettingshausen, D. Dixon, A. Schoekel, C. Roth, P. Altantsog, D. Sangaa and C. Ganzori, *J. Nanomater*, 2010, **2010**, 1-9.
31. M. Cargnello, V. V. T. Doan-Nguyen, T. R. Gordon, R. E. Diaz, E. A. Stach, R. J. Gorte, P. Fornasiero and C. B. Murray, *Science*, 2013, **341**, 771-773.
32. P. G. N. Bouchenafa-Saib, P. Verhasselt, F. Addoun, V. Dubois, Appl. Catal. A: Gen. 2005, 286, 167–174., *Appl. Catal. A: Gen.*, 2005, **286**, 167-174.
33. X. Yu, M. Wang and H. Li, *Appl. Catal. A: Gen.* , 2000, **202**, 17-22.
34. R. Giordano, P. Serp, P. Kalck, Y. Kihn, J. Schreiber, C. Marhic and J.-L. Duvail, *Eur. J. Inorg. Chem.* , 2003, **2003**, 610-617.
35. C.-H. Li, Z.-X. Yu, K.-F. Yao, S.-F. Ji and J. Liang, *J. M. Cat. A: Chem.*, 2005, **226**, 101-105.
36. P. Sangeetha, K. Shanthi, K. S. Rama Rao, B. Viswanathan and P. Selvam, *Appl. Catal. A: Gen.*, 2009, **353**, 160-165.
37. N. Arora, A. Mehta, A. Mishra and S. S. Basu, *App. Clay Sci.*, 2018, **151**, 1-9.
38. Y. Chen, L. Li, L. Zhang and J. Han, *Colloid Polymer Sci.*, 2018, **296**, 567-574.
39. S. Sadjad, M. M. Heravi and R. M., *Carbohydr Polym.*, 2018, **185**, 48-55.
40. S. Sadjadi, M. M. Heravi and M. Daraie, *J. Mol. Liq.* , 2017, **231**, 98–105.
41. S. Sadjadi, M. M. Heravib, M. Malmir and B. Masoumi, *Appl. Organomet. Chem.*, DOI: 10.1002/aoc.4113.
42. S. Sadjad and M. Atai, *Appl. Clay. Sci.*, 2018, **153**, 78-89.
43. S. Sadjad, M. M. Heravi and M. Malmir, *Carbohydr Polym.*, 2018, **186**, 25-34.
44. S. Sadjad, *Appl. Organomet. Chem.*, DOI: 10.1002/aoc.4211.
45. J. Zhang, D. Hao, H. Lu, W. Leng, J. Gui and Y. Gao, *Materlas lett.*, 2016, **126**, 259-262.
46. Y. Zou, X. Wang, Y. Ai, Y. Liu, Y. Ji, H. Wang, T. Hayat, A. Alsaedi, W. Hu and X. Wang, *J. Mater. Chem. A* 2016, **4**, 14170-14179 .
47. S. Sadjadi, M. M. Heravi and M. Malmir, *Res. Chem. Intermed.*, 2017, In press.
48. H. Zhu, M. L. Du, M. L. Zou, C. S. Xu and Y. Q. Fu, *Dalton Trans.*, 2012, **41**, 10465–10471.
49. P. Yuan, P. D. Southon, Z. Liu, M. E. R. Green, J. M. Hook, S. J. Antill and C. J. Kepert, *J. Phys. Chem. C* 2008, **112**, 15742–15751.
50. S. Mallik, S. S. Dash, K. M. Parida and B. K. Mohapatra, *J. Colloid Interface Sci.*, 2006, **300**, 237–243.
51. S. Bordeepong, D. Bhongsuwan, T. Pungrassami and T. Bhongsuwan, *Songklanakarin J. Sci. Technol*, 2011, **33**, 599-607.
52. L. Zatta, J. E. F. da Costa Gardolinski and F. Wypych, *Appl. Clay Scie.*, 2011, **51**, 165–169.
53. U. R. Pillai and E. Sahle-Demessie, *J. Mol. Catal. A.*, 2004, **222**, 153-158.
54. A. Lazzarini, E. Groppo, G. Agostini, E. Agostini, F. Giannici, G. Portale, A. Longo, R. Pellegrini and C. Lamberti, *Catal. Today*, 2017, **283**, 144-150.
55. G. Giachi, W. Oberhauser, M. Frediani, E. Passaglia, L. Capozzoli and L. Rosi, *J. Polym. Sci. A*, 2013, **51**, 2518–2526.
56. S. F. Zhong, *Turk. J. Chem.*, 2017, **41**, 773-783.
57. M. Vilar and M. Navarro, *Electrochimica Acta*, 2012, **59**, 270– 278.
58. A. R. Kiasat and S. Sayyahi, *Catal. Commun.* , 2010, **11**, 484–486.
59. F. Wyrwalski, B. Léger, C. Lancelot, A. Roucoux, E. Monflier and A. Ponchel, *Appl. Catal., A.*, 2011, **391**, 334–341.
60. N. T. Thanh Chau, J. P. Guégan, S. Menuel, M. Guerrero, F. Hapiot, E. Monflier, K. Philippot, A. Denicourt-Nowicki and A. Roucoux, *Appl. Catal., A.*, 2013, **467**, 497–503.
61. A. Nowicki, Y. Zhang, B. Le´ger, J.-P. Rolland, H. Bricout, E. Monflier and A. Roucoux, *Chem. Commun.*, 2006, DOI: 10.1039/b512838b, 296–298.
62. T.-L. Cui, W.-Y. Ke, W.-B. Zhang, H.-H. Wang, X.-H. Li and J.-S. Chen, *Angew. Chem. Int. Ed.* , 2016, **55**, 1 -6.
63. M. Lamblin, L. Nassar-Hardy, J.-C. Hierso, E. Fouquet and F.-X. Felpin, *Adv. Synth. Catal.* , 2010, **352**, 33 -79.

Pd nanoparticles immobilized on halloysite decorated with cyclodextrin modified melamine-based polymer: a promising heterogeneous catalyst for hydrogenation of nitroarenes

Samahe Sadjadi[*a], Maryam Akbari[b], Eric Monflier[c], Majid, M. Heravi[b], Bastien Leger[c]